JOURNAL OF APPLIED ELECTROCHEMISTRY 18 (1988) 463–468

Electrochemical etch-stop control for silicon structures containing electronic components

R. L. GEALER, R. H. HAMMERLE, H. KARSTEN*, H. S. WROBLOWA
Ford Motor Company, Research Staff, Dearborn, MI 48121, USA

Received 2 July 1987; revised 20 November 1987

A predictive analysis of the feasibility of electrochemical etch-stop control in the fabrication of some silicon sensors was validated experimentally. The application is for sensors with thin silicon structures containing electronic components, such as cantilever accelerometers and diaphragm pressure gauges with strain gauges in the surface to detect deflection. Such structures are formed by deep anisotropic etching of silicon. Since the depth of the etch determines the thickness of the cantilever or diaphragm, the ability to stop the etching precisely is critical. Accurate etch-stop control can be accomplished by electrochemical passivation of an n-type epitaxial layer on a p-type silicon wafer, where the epi layer thickness becomes that of the diaphragm or cantilever. The analysis shows that passivation of the epi layer can be maintained even underneath the electronic components for conditions which allow etching of the p-type silicon substrate. Therefore, electrochemical etch-stop control appears feasible in most practical sensor designs.

1. Introduction

In a previous publication [1] an analysis was given of the current and potential distributions along resistive electrodes. The need to revise and expand the simple theory [2] arose in connection with the fabrication of miniature sensor devices. Thin silicon structures produced by anisotropic deep wet etching of single crystals are often required, e.g. for pressure sensor diaphragms [3] or accelerometer cantilever paddles [4]. The methods to control the etch depth, and hence the silicon structure thickness, include: timing a known etch rate in a controlled system; etch stop at a highly doped boron layer in the silicon [5] and electrochemical passivation at a p–n junction in the silicon [6]. Each method has potential applications, but the electrochemical passivation at a p–n junction offers the more promising approach when very accurate etch depths are required and when electronic devices such as implanted piezoresistors must be incorporated into the silicon remaining after deep etching.

Electrochemical passivation at a p–n junction can be used to control the etch depth in the following way. A p-type silicon wafer is selected with an n-type epitaxial (epi) layer whose thickness is suitable for the desired device, e.g. a diaphragm for a pressure sensor (*cf.* Fig. 1a). Ideally, the epi layer is coated with a metal film to which a positive voltage is applied which is sufficient to passivate the n-layer but too low to passivate the p-layer across the barrier presented by the p–n junction. The wafer is immersed in the electrolyte. Etching of the substrate occurs at the opposite face of the wafer where the desired portions of the surface are protected by a photolithographically patterned mask. Etching stops at the n-type epi layer which passivates upon exposure to the electrolyte [6].

In this configuration, the ohmic drop through the thin n-type epi layer is usually negligible as compared to the cell voltage and therefore the electrode need not be considered resistive. However, in many practical applications the epi layer cannot be completely coated with a metal film, because of electronic components incorporated into the diaphragm or cantilever. Figure 1b depicts a schematic cross section of such a device. The electronic components are covered with a protective coating such as silicon nitride, which insulates the current-carrying metal film from the silicon under the protected component. Thus, for passivation to occur underneath these devices, the current must flow from the metal adjoining them on the epi surface along the epi layer to all points underneath these devices and then into the electrolyte. In this case the epi layer becomes a resistive electrode.

The length of the passivated part of the epi layer depends on its resistivity and on the applied potential. Analysis of this dependence has been given in a separate publication [1]. It allows an evaluation to be made of the size of electronic devices for which the passivation can still occur uniformly at the p–n junction underneath them. The experimental verification of the predictive model [1] is described below.

2. Experimental details

The test samples consisted of rectangular pieces of (100)-oriented 260–450 μm single crystal silicon wafers, both p- and n-type, having resistivities ranging from 1.5 to 45 Ω cm. The wafers were polished on one face. The polished face was metalized with a 0.1 μm

* *Present address*: Dow Chemical Company, Midland, MI 48667, USA.

0021-891X/88 $03.00 + .12 © 1988 Chapman and Hall Ltd.

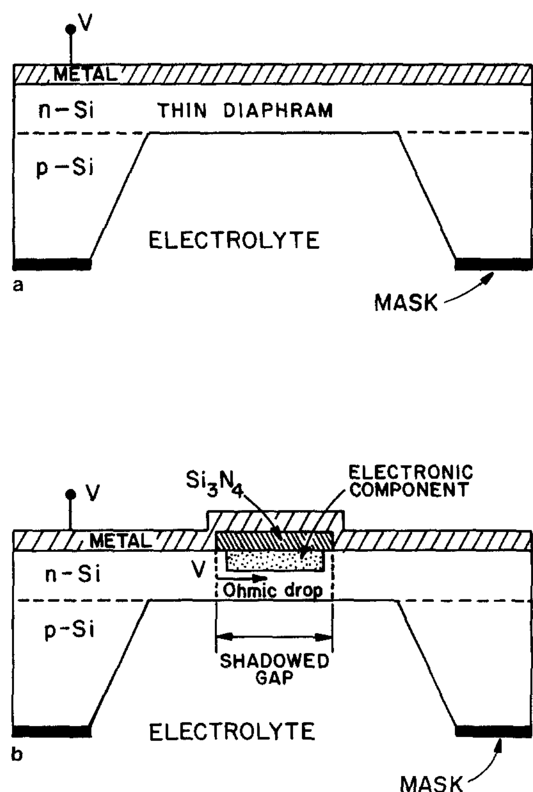

Fig. 1. (a) Schematic cross section of a silicon diaphragm with thickness controlled by electrochemical etch stop at a p–n interfacial junction. (b) Schematic cross section of a silicon diaphragm incorporating electronic component which can inhibit electrochemical etch stop due to ohmic drop in its shadow.

layer of vacuum evaporated gold deposited over a 0.1 μm layer of sputtered chromium in one of the patterns shown schematically in Fig. 2. These samples were vertically mounted opposite a platinum black counterelectrode mounted in a Teflon holder. Electrical contact was made with a gold contact pad clamped against the upper horizontal metalized strip on the sample. The samples were immersed, to a depth as depicted in Fig. 2 and with both faces exposed, in an electrolyte consisting of aqueous ethylenediamine–pyrocatechol (EDP) etching solution at 100° C. The EDP components were in the proportion 100 ml ethylenediamine : 16 g pyrocatechol : 32 ml water.

The three-electrode cell consisted of a Pyrex vessel equipped with a reflux condenser to avoid loss of volatile electrolyte components, a gas inlet for purging the electrolyte with nitrogen, a magnetic stirrer and a thermostatically controlled heating mantle. Potentials were measured against the saturated calomel electrode (SCE). Using standard potentiostatic equipment, the sample studied was polarized at a given applied potential, V_L, as shown in Fig. 2. A horizontal potential distribution, which results from the ohmic drop in the resistive silicon electrode, originates at the vertical metalized strip. At values of V_L more anodic than the passivation potential, V_p, a part of the silicon surface passivates and prevents silicon dissolution for a lateral distance $(L - y_p)$ from the metalized strip. Beyond that distance the dissolution rate is determined by the local overpotential.

The sample was immersed for 15 min to establish an easily observable etch profile. A schematic cross section of an electrode depicting the passivated/etched profile is shown in the bottom portion of each sample configuration in Fig. 2. The passivated distances were determined by measuring the sample profiles with a stylus type profilometer. No significant differences were observed between the etched profiles on the metalized and the non-metalized faces. This was expected since the potential distributions on both faces, at some small distance away from the metalized strip, would be nearly the same due to the negligible resistance through the thin silicon layer. The sample would thus behave electrically as if it were split into two samples along the mid-plane, each having half the thickness. There was a slight tendency for the surface which faced the counterelectrode to have greater passivated distance, but the differences were small and not considered highly significant.

For metalization pattern (a) in Fig. 2 the voltage was applied from both sides of the centerline, resulting in a symmetrical potential distribution about this line.

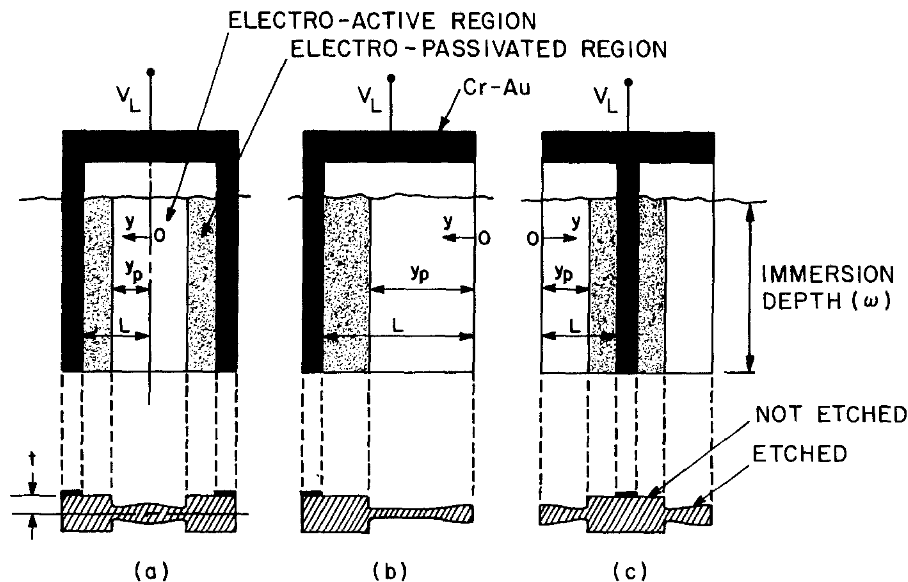

Fig. 2. Metalization patterns applied to silicon electrode surfaces.

Thus, no current crossed the centerline. This configuration is equivalent to the sample being split along the centerline giving two separate pieces of silicon, each with exposed length L. Therefore, passivated distance data could be obtained on both sides of the centerline. Profilometer scans were done horizontally at three positions across each face. Generally, for samples with configurations (a) and (c), the average of 12 passivation distance measurements was determined (three scans, both sides of center, both faces), while for samples with configuration (b), six measurements were averaged (three scans, both faces).

Polarization curves required to establish the values of the passivating potential and current density were obtained in separate experiments, with thin silicon electrodes that were backed by a uniform gold coating (with a chromium interlayer) over the polished face, so that the entire electrode could be considered equipotential. Otherwise the cell geometry was identical with that used in the determinations of passivated lengths. The metalized face of the immersed part of the electrode was coated with a layer of silicone rubber to prevent current flow at the gold/electrolyte interface. The samples were mounted vertically in the previously described holder having the non-metalized silicon surface facing the Pt gauze counterelectrode. The samples were immersed in the EDP solution at 110° C, and their potential varied in the anodic direction over the desired range using standard potentiostatic and function generating equipment. Sweep rates of 33 and $100\,\mathrm{mV\,min^{-1}}$ gave similar results, so most experiments were done at $100\,\mathrm{mV\,min^{-1}}$.

3. Results and discussion

Typical plots showing the polarization curves for samples of two silicon materials in the electrochemical system described above are presented in Fig. 3. The potentials for the p-type silicon have been corrected for a small Schottky barrier potential drop between the metalized film and the silicon surface amounting at most to 0.03 V at the highest current density. The Schottky barrier potentials were determined in separate experiments in air at 110° C by measuring the voltage drop through the thickness of the p-type silicon samples, metalized on both faces, as a function of current density. There was no potential barrier between the metalized film and the n-type silicon surfaces.

Polarization curves exemplified in Fig. 3 for n- and p-silicon samples exhibit ohmic behavior:

$$\delta V/\delta i = r \tag{1}$$

where V is potential, i is the current density and r is the resistance ($\Omega\,\mathrm{cm^2}$) between the test and reference electrodes. The resistance is most probably due to the presence of a prepassive film on silicon.

Analysis of the current and potential distribution along a resistive electrode given previously [1] for the case of the linear (low overpotential) approximation must be slightly revised. The model and equations

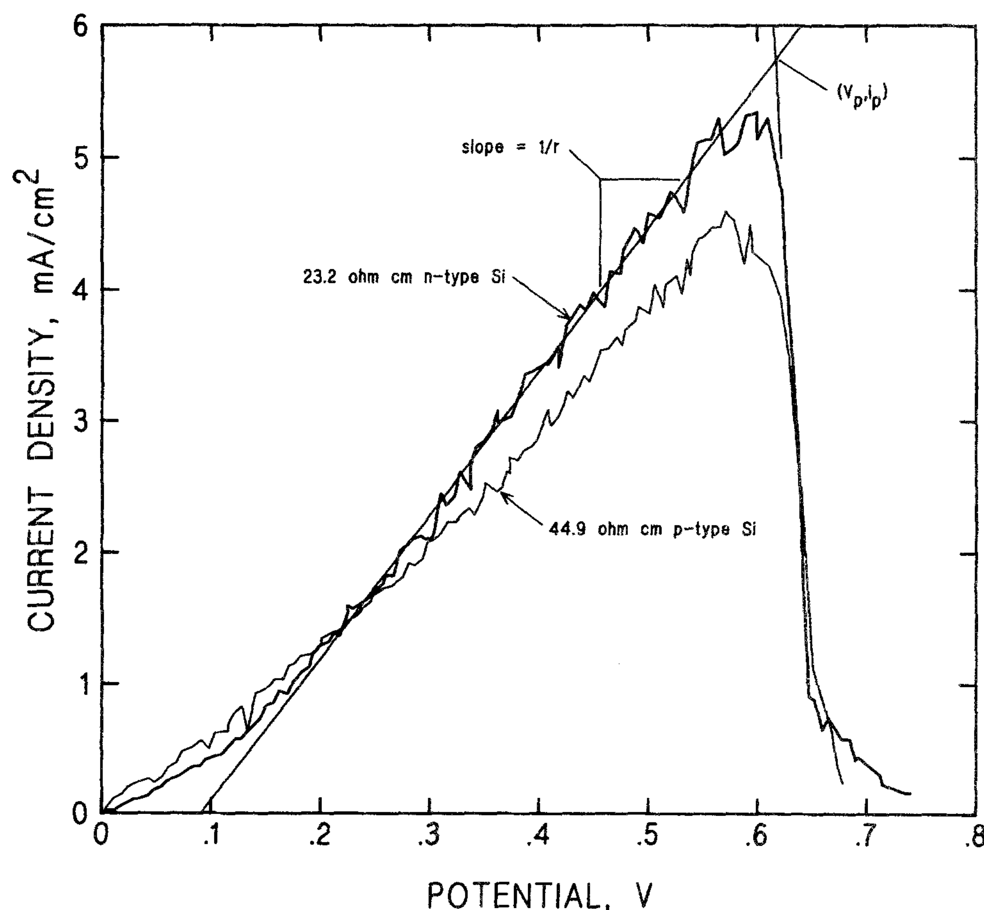

Fig. 3. Current density vs potential relative to open circuit.

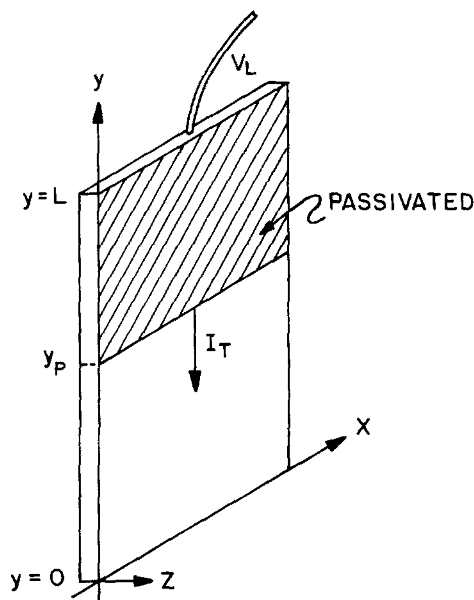

Fig. 4. Schematic diagram of a partially passivated model electrode.

retain their validity, but certain constants have a different meaning. Consider a model (Fig. 4) of a passivating flat electrode of specific resistivity ϱ, length L, width w and thickness t. The upper part of the electrode between points $y = L$ and $y = y_p$ is passivated. Under conditions presently considered, the local current density, i_y, obtained by integration of Equation 1 is:

$$i_y = \text{const.} + V_y/r, \quad (2)$$

and the current increment, $I' \equiv \delta I/\delta y$, at a point y is given by

$$I'y \equiv i_y w \approx \text{const.} + V_y w/r \quad (3)$$

Equation 3 has a similar mathematical form to Equation 18 of Ref. [1]. Thus, the mathematical treatment of the present case is similar to that given there, which led to the expression (31) for the 'excess' potential, i.e. the difference between the applied potential, V_L, and passivating potential, V_p:

$$V_L - V_p = (i_p\varrho/kt)(L - y_p)[\tanh(ky_p)] \quad (4)$$

In Equation 4 the constant $k = (\varrho/rt)^{1/2}$.

In order to establish the predictive value of the passivating resistive electrode model, experimentally measured passivation distances were compared to calculations made using Equation 4. The passivating potential, V_p, and the passivating current density, i_p, were obtained from plots such as Fig. 3. The slopes of the plots correspond to $1/r$ (*cf.* Equation 1) from which the coefficient $k = (\varrho/rt)^{1/2}$ may be determined. The values of V_p and i_p were taken at the intersection of the straight trend line with the extension of the line defining the steep decrease in current density, as shown in Fig. 3.

Table 1. Experimental coefficients

Silicon dopant type		i_p *(mA cm^{-2})*	*1/r (Ω^{-1} cm^{-2})*
n	mean (8)	5.65	0.0116
	(SD)	(0.49)	(0.0007)
p	mean (7)	4.79	0.0099
	(SD)	(0.26)	(0.0011)

As was previously discussed [1] the function Equation 4 has a maximum as y_p decreases from L to 0, and any increment of the applied potential above that maximum will result in the passivation of the entire electrode. The value of y_p for this maximum can be found by equating the first derivative of Equation 4 to zero; this yields

$$k(L - y_{p,\max}) = 0.5 \sinh(2ky_{p,\max}) \quad (5)$$

Voltammetric curves exemplified in Fig. 3 were generated for eight samples of n-type silicon (including samples having resistivities of 23.2 and 1.5 Ω cm) and seven samples of p-type silicon (including samples having resistivities of 44.9 and 4.0 Ω cm). The mean values of passivation current density, i_p, and slope, $1/r$, derived from these plots (*cf.* Table 1) are slightly greater for the n-type than for the p-type silicon, although the ranges of uncertainty nearly overlap. Using these experimentally determined coefficients and Equation 3, passivated distances $(L - y_p)$ were then calculated for the geometries shown in Fig. 2 at values of excess potential for which experiments were carried out.

Experimental passivated distances were determined from the profilometer scans of samples etched under the given applied potential values. Figure 5 exemplifies a profilometer scan in the y direction of the metalized face of a sample with the metalization pattern shown in Fig. 2a. The edges of the very thin film of metal (0.2 μm) are seen as small steps on either side

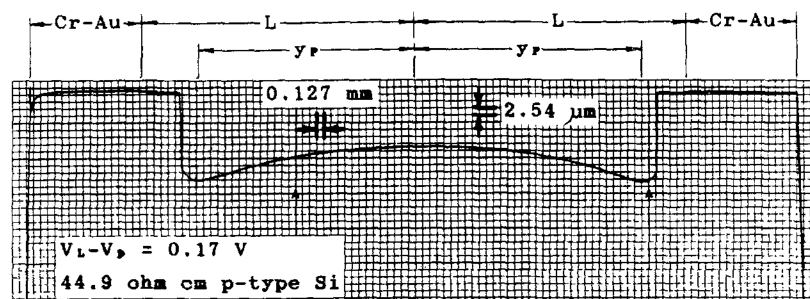

Fig. 5. Profilometer trace of a partially passivated electrode.

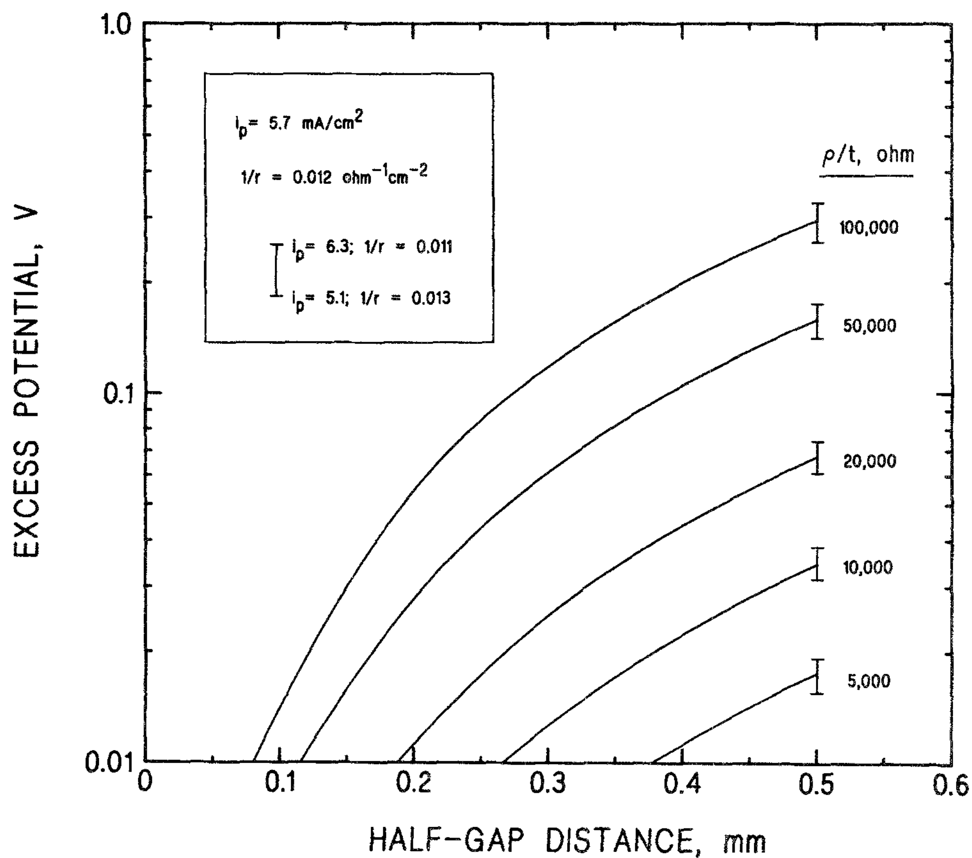

Fig. 6. Excess potential requirement for shadowed gap passivation.

of the sample. For comparison to passivated distances predicted by the linear model, the position at which passivation occurred was designated to be where the current density was maximum (i_p). Since the etch rate increases with current density, this position was taken to be where the etch depth was maximum, as shown in Fig. 5. Closer to the metalized strip, the etch rate and current density decreased steeply as the value of the passivation potential was exceeded.

The experimental and predicted passivated distances are compared in Table 2. The validity of the model is supported by the reasonably good agreement shown. Note that in four of the experiments the excess potential was high enough that passivation to a distance $(L - y_{p,max})$, and hence passivation of the entire surface, was predicted [1]. In three of the cases, the prediction was correct.

The passivating resistive electrode model [1] has been used to predict the excess potential, $V_L - V_p$, required at the edge of a shadowed gap (as depicted in Fig. 1b) to ensure that passivation would occur at the center of the gap, or conversely, to predict how large a gap may be passivated with a given excess potential. This was done by calculating the excess potential required to passivate the sample to a distance $(L - y_{p,max})$ using Equations 4 and 5 which would then result in passivation for the whole distance L. Note that one need only apply sufficient potential to

Table 2. Comparison of predicted and experimental passivation distances

Resistivity-dopant type, ϱ (Ωcm)	*Half thickness, t (μm)*	*Metalization pattern (Fig. 2)*	*Exposed length, L (mm)*	*Excess potential, $V_L - V_p$ (V)*	*Passiv. distance (pred.), $L - y_p$ (mm)*	*Passiv. distance (exp.), $L - y_p$ (mm)*	*SD (mm)*
23.2-n	130	a	5.1	0.21	1.0	1.0	0.2
		b	11.7	0.91	4.1	3.3	0.2
44.9-p	225	a	5.0	0.17	0.8	1.1	0.2
		a	5.0	0.69	5.0*	3.0	0.3
		a	5.0	0.79	5.0*	5.0	
		b	7.7	0.68	3.3	2.3	0.2
		c	7.7	0.64	3.1	2.4	0.4
		b	9.7	0.65	3.1	2.4	0.2
4.0-p	193	a	5.0	0.10	5.0*	5.0	
1.5-n	196	a	5.0	0.06	5.0*	5.0	

* $(V_L - V_p)$ exceeds the value calculated using Equations 4 and 5; therefore, the model predicts that the entire electrode length is passivated.

passivate half the gap to the center, since the potential is applied from both sides. Hence, for this configuration, the length L to be passivated is the half-gap.

The predicted relationship between excess potential and the half-gap distance passivated is presented in Fig. 6 for n-type silicon having a range of resistivity-to-thickness ratios. For each curve, bars are shown at 0.5 mm half-gap which indicate the predicted excess potential variation for $\pm 10\%$ errors in i_p and $1/r$. For a resistivity-to-thickness ratio of silicon as high as 100 000 Ω corresponding, say, to a 50 Ω cm, 5 μm thick layer, the excess potential required to passivate a 1 mm gap (from both sides) is only 0.3 V. Thus, there should be no difficulty in passivating an insulated gap in most situations of practical interest.

References

[1] H. S. Wroblowa, R. H. Hammerle and R. L. Gealer, *J. Appl. Electrochem.* **18** (1988) 469.

[2] B. E. Conway and E. Gileadi, *Can. J. Electrochem.* **41** (1963) 2447.

[3] S. K. Clark and K. D. Wise, *IEEE Trans. Electron Dev.* **ED-26** (1979) 1887.

[4] L. M. Roylance and J. B. Angell, *ibid.* (1979) 1911.

[5] I. Barycka, H. Teterycz and Z. Znamirowski, *J. Electrochem. Soc.* **126** (1979) 345.

[6] T. N. Jackson, M. A. Tischler and K. D. Wise, *IEEE Electron Dev. Lett.* **EDL-2** (1981) 44.